





Cite this: *Phys. Chem. Chem. Phys.*,
2023, **25**, 27914

Received 28th June 2023,
Accepted 16th September 2023

DOI: 10.1039/d3cp03042c

rsc.li/pccp

Precision spectroscopy of molecular hydrogen

Qian-Hao Liu, Yan Tan,* Cun-Feng Cheng * and Shui-Ming Hu *

Precision measurements on the hydrogen molecule are of fundamental importance in understanding molecular theory. Comparison of accurate experimental data and theoretical results are used to test the quantum electrodynamics theory and determine physical constants used in the calculation. We review recent advances and perspectives in the precision spectroscopy of molecular hydrogen, representing state-of-the-art molecular spectroscopy methods and cutting-edge high-precision calculations.

1. Introduction

The hydrogen molecule, as one of the simplest and calculable two-electron systems, is a benchmark for quantum theory of chemical bonds. In 1927, Heitler and London calculated the dissociation energy of the electron ground state by solving the Schrödinger equation of the hydrogen molecule.¹ The work successfully revealed the nature of molecular bonds based on quantum mechanics, which announced the beginning of modern quantum chemistry. In principle, energy levels of the hydrogen molecule (and its isotopologues) can be calculated with high precision based only on quantum electrodynamics (QED) and some fundamental physical constants, such as the Rydberg constant R_y , the fine structure constant α and the proton-to-electron mass ratio m_p/m_e . In the past, it was thought that the calculated energy levels of the hydrogen molecule could hardly reach a precision comparable to that of the hydrogen atom. The main difficulty comes from calculating QED corrections up to the order of $\alpha^4 R_y$ and the exact solution of the non-relativistic Schrödinger equation for the hydrogen molecule. However, recent progress in both issues indicates that the vibration-rotation state energies in the electronic ground state of the hydrogen molecule could be calculated to the order of 10^{-6} cm^{-1} .^{2,3} At this precision, the comparison between theoretical and experimental results can be used to test the QED theory,⁴ determine fundamental physical constants,^{3,5} and even search for new physics beyond the Standard Model.^{6,7} Moreover, due to the overlap of the electron orbital with the nuclei, the finite-nuclear-size (FNS) effect also yields a measurable contribution to the energies of molecular

hydrogen. Consequently, precision spectroscopy of molecular hydrogen provides an alternative way to solve the long-standing “proton size puzzle”.⁸

As a homonuclear diatomic molecule, H_2 (and also D_2) has no electric dipole moment transition (E1) in its electronic ground state, but very weak electric quadrupole moment transitions (E2). Measurement of absorption spectra of H_2 has been a challenging and interesting target for spectroscopists in the past decades. Hydrogen and its isotopologues are classical test species for theoretical calculations not only for transition frequencies and energy levels but also for line intensities. The quadrupole transition probabilities of hydrogen can be calculated with highly accurate electronic potential energy curves and electric quadrupole moment curves which makes it an extremely tractable quantum mechanical subject. There could be significant deviations as expected between the calculated state energies for high V and J states and the refinement is performed typically through an empirical fit to experimentally accurate state energies. The recent calculations of Roueff *et al.* provide the full infrared spectrum of molecular hydrogen at an unprecedented accuracy in which the quadrupole moment function was obtained using the Born–Oppenheimer potential energy including several higher-order correction terms.⁹ For the first time, the emission probabilities of both electric quadrupole and magnetic dipole transitions were derived in this work. Moreover, the hydrogen molecule is also the most abundant neutral molecule in the universe and dominates the atmosphere of gas giants in the solar system and beyond. Laboratory-measured spectral data of the hydrogen molecule, including transition frequencies, intensities, and related temperature-/pressure-dependent spectroscopic parameters, are the basis for modeling the planetary atmospheres.^{10,11} Spectral analysis based on these spectroscopic parameters led to the previous discovery that hydrogen is the main component of the

Department of Chemical Physics, University of Science and Technology of China, Hefei, 230026, China. E-mail: tanyan@ustc.edu.cn, cfcheng@ustc.edu.cn, smhu@ustc.edu.cn

atmospheres of Jupiter, Saturn, and other planets,^{12,13} and more accurate data is demanded to improve the analysis.

It is well known that the Voigt profile leads to significant deviations concerning spectra with high signal-to-noise ratios, hence IUPAC recommends the Hartmann-Tran profile (HTP) to interpret line profiles of high-resolution spectroscopic transitions,¹⁴ and the HITRAN database has implemented non-Voigt profiles of H₂ since HITRAN2016.^{15,16} However, the implementation of the HTP requires taking into account various effects such as Doppler broadening, pressure-induced broadening and shifting, and additional collisional effects which include Dicke narrowing, speed-dependent collisional broadening and shifting, the correlation between velocity-changing and dephasing or state-changing collisions. There are strong correlations between these parameters in adopting HTP in fitting experimental spectra in various studies and applications.¹⁷ Doppler-limited spectra of molecular hydrogen become an ideal test case for the line shape theory since both velocity-changing and speed-dependent effects resulting from molecular collisions are exceptionally pronounced here.^{18,19} Moreover, absorption lines of hydrogen are well isolated which excludes the influence of other nearby transitions, and *ab initio* line-shape calculations from quantum mechanical scattering or classical molecular dynamic simulations (CMDs) for hydrogen have been established.^{20,21} Therefore, high-resolution spectroscopy of the hydrogen molecule also presents an excellent test ground for line profile models.

Here we review the latest progress in precision spectroscopy of the hydrogen molecule. The second section introduces the theories and high-precision calculation of energy levels of the hydrogen molecule. The third and fourth sections present spectroscopy of the vibration-rotation transitions in the electronic ground state and electronic transitions, respectively. Conclusions and perspectives are given in the last section.

2. Theoretical energy levels

In 1927, almost one century ago, Heitler and London¹ first derived the dissociation energy of the hydrogen molecule H₂ using the variation method, but the result has a considerably large deviation, about 2 eV less than the experimental value. Several years later, James and Coolidge^{22,23} dramatically improved the calculation accuracy and gave a value of $D_0 = 4.454(13)$ eV, which is only 0.024 eV higher than the present accurate value. In the 1960s, Kołos and Wolniewicz took systematic calculations of rovibrational energy levels in the electronic ground state of H₂ (and other isotopologues) within the framework of the adiabatic approach.²⁴ By taking into account adiabatic and relativistic corrections, they obtained a dissociation energy of $D_0 = 36117.4$ cm⁻¹ for H₂ with uncertainties below 1 cm⁻¹.^{25,26} However, the value was 3.8 cm⁻¹ larger than the experimental value given by Herzberg and Monfils in 1961,²⁷ which contradicts the variation principle. The puzzle remained for one decade until Herzberg²⁸ and Stwalley²⁹ reported new experimental values, which were

36 118.3 cm⁻¹ and 36 118.6(5) cm⁻¹, respectively. Kołos, Wolniewicz and their colleagues continued to improve *ab initio* calculations of the energy levels of the hydrogen molecule.³⁰⁻⁴⁸ In 1993, Kołos and Rychlewski reported⁴⁹ a theoretical dissociation energy of 36 118.049 cm⁻¹ for the ground state H₂, and the value reported by Wolniewicz^{41,43} was 36 118.069 cm⁻¹. After that, high-order relativistic and QED corrections were included in the calculation, and the precision of theoretical calculations of the energy levels of molecular hydrogen was successively improved in recent two decades by Pachucki and his colleagues.^{2,3,5,50-62}

Energies of the hydrogen molecule, as of any light bounded system, can be expanded⁶³ in powers of the fine structure constant α ,

$$E(\alpha) = \alpha^2 E^{(2)} + \alpha^4 E^{(4)} + \alpha^5 E^{(5)} + \alpha^6 E^{(6)} + \alpha^7 E^{(7)} + \dots \quad (1)$$

The leading term $E^{(2)}$ is the non-relativistic energy, which has been calculated to a precision at the 10⁻⁸ cm⁻¹ level for the ground electronic state⁵³ using the explicitly correlated exponential (ECE) basis functions. For the calculation for a highly excited state, the nonadiabatic perturbation theory (NAPT) gives an accuracy of about 10⁻⁴ cm⁻¹.^{64,65}

The next coefficient $E^{(4)}$ is the leading relativistic correction. It has been calculated for the ground electronic state ($1^1\Sigma_g^+$) using the nonadiabatic explicitly correlated Gaussian (ECG) functions with a precision below 10⁻⁶ cm⁻¹.⁶¹ The excited state can be calculated with NAPT to about 10⁻⁶ cm⁻¹. Regarding the leading quantum electrodynamics correction $E^{(5)}$, it has been calculated within the Born–Oppenheimer (BO) approximation, which contributes the leading uncertainty of 2×10^{-4} cm⁻¹ to the calculated result. The next-order correction $E^{(6)}$ is also known within the BO approximation, giving an uncertainty of the order of 10⁻⁶ cm⁻¹.³ The last term $E^{(7)}$ has been estimated according to the atomic hydrogen values, and the uncertainty is at the order of 10⁻⁵ cm⁻¹, giving the second largest contribution to the uncertainty budget. Further corrections like the finite nuclear size have been estimated with an accuracy below 10⁻⁶ cm⁻¹.

Using the NAPT method, Pachucki and his colleagues calculated the ro-vibrational state energies^{52,66,67} and dissociation energy^{51,63} of molecular hydrogen in the electronic ground state with an accuracy of about 0.001 cm⁻¹. The dissociation energy of H₂ was calculated to be 36 118.0695(10) cm⁻¹, agreeing well with the experimental result of 36 118.0696(4) cm⁻¹ given by Liu *et al.*⁶⁸ The independent calculation without using the Born–Oppenheimer approximation is also helpful to check both theoretical and experimental results.⁶⁹ The list of transitions of H₂ and HD given in the HITRAN database¹⁵ is also based on these calculated results. The most recent⁵⁹ theoretical D_0 value of H₂ is 36 118.069632(26) cm⁻¹, and respective values⁶² for D₂, T₂, HD, HT and DT are given in Tables 1 and 2. The theoretical treatment for HD is the same as that for H₂ and D₂, a much larger (more than 3 σ) discrepancy between the experimental and theoretical dissociation energies of HD⁶² is found and later resolved with carefully analyzing the *g/u*-symmetry breaking of the Rydberg state during the process of obtaining the dissociation energy.⁷⁰ On the other hand, the comparison of the vibrational transition energy between theory

Table 1 Some precise frequencies of H₂, D₂, and T₂. The Raman, Doppler, Beam, CARS and Lamb dip mark the Raman spectroscopy, Doppler-limited spectroscopy, beam experiment, coherent anti-Stokes Raman spectroscopy and Lamb dip measurement, respectively

$(V, N') \leftarrow (V, N)$	Frequency, MHz	Note	Ref.
H₂			
(0, 1) \leftarrow (0, 0)	3 552 145.28(4)	Calc.	73
	3 552 144.0(15)	Exp.	74
	3 552 145.0(30)	Exp.	75
(1, 0) \leftarrow (0, 0)	124 748 622.0(8)	Calc.	73
	124 748 629.1(45)	Exp.	76
(1, 1) \leftarrow (0, 1)	124 571 373.89(78)	Calc.	77
	124 571 374.73(31)	Exp., Raman	78
(2, 2) \leftarrow (0, 0)	252 016 358.5(15)	Calc.	77
	252 016 361.16(6)	Exp., Doppler	79
(2, 3) \leftarrow (0, 1)	257 947 882.1(15)	Calc.	77
	257 947 884.67(3)	Exp., Doppler	79
(3, 5) \leftarrow (0, 3)	376 531 814.7(24)	Calc.	73
	376 531 814.1(16)	Exp., Doppler	80
$D_0^{N=0}$	1 082 792 487.3(8)	Calc.	59
	1 082 792 486.5(9)	Exp.	81
$D_0^{N=1}$	1 079 240 344.3(8)	Calc.	59
	1 079 240 344.2(7)	Exp.	82
	1 079 240 342.4(3)	Exp.	74
D₂			
(1, 0) \leftarrow (0, 0)	89 746 381.31(27)	Calc.	83
	89 746 381.7(45)	Exp.	76
(1, 3) \leftarrow (0, 1)	94 925 100.0(4)	Calc.	73
	94 925 100.487(17)	Exp., Beam	84
(2, 2) \leftarrow (0, 0)	180 914 269.04(72)	Calc.	73
	180 914 269.55(30)	Exp., Doppler	85
(2, 4) \leftarrow (0, 2)	187 104 298.90(63)	Calc.	83
	187 104 300.04(39)	Exp., Doppler	86
$D_0^{N=0}$	1 101 688 187.4(8)	Calc.	62
	1 101 688 185.6(6)	Exp.	87
T₂			
(1, 0) \leftarrow (0, 0)	73 883 975.7(18)	Calc.	88
	73 883 969.4(200)	Exp., CARS	89
(1, 1) \leftarrow (0, 1)	73 849 326.0(18)	Calc.	88
	73 849 320.3(126)	Exp., CARS	89
$D_0^{N=0}$	1 110 086 390.5(8)	Calc.	62

and experiment shows a disagreement about 2 times standard deviation,^{71,72} indicating more investigations are necessary. As a summary, some of the recently calculated ro-vibrational frequencies are also given in Tables 1 and 2.

If a precision of 10^{-7} cm⁻¹ could be achieved in the calculation, uncertainties in present fundamental constants like the proton-to-electron mass ratio or the proton charge radius will play a role.¹⁰⁰ Therefore, precise energies of molecular hydrogen, alternative to atomic hydrogen, can be explored to determine these constants from properly selected transitions. The dependence between a particular transition frequency ν and a physical constant C could be interpreted with a coefficient:

$$\frac{\delta\nu}{\nu} = \beta \frac{\delta C}{C} \quad (2)$$

As an example, the β coefficients for the $R_2(1)$ transition ($J=2 \leftarrow 1$, $V=2 \leftarrow 0$) of HD have been calculated by Pachucki and Komasa,¹⁰¹ and they are given in Table 3 together with the CODATA 2018¹⁰² recommended constants. If the theoretical calculation agrees with the experimental measurement with an

Table 2 Some precise frequencies of HD, HT, and DT. The experimental methods are marked as in Table 1

$(V, N') \leftarrow (V, N)$	Frequency, MHz	Note	Ref.
HD			
(0, 1) \leftarrow (0, 0)	2 674 986.073(18)	Calc.	83
	2 674 986.094(24)	Exp., Lamb dip	90
(1,0) \leftarrow (0, 0)	108 889 429.4(6)	Calc.	83
	108 889 433.0(66)	Exp.	76
(1, 1) \leftarrow (0, 0)	111 448 814.5(6)	Calc.	73
	111 448 815.477(13)	Exp., Beam	91
(2, 2) \leftarrow (0, 1)	214 905 333.3(11)	Calc.	77
	214 905 335.185(20)	Exp., Doppler	92
(2, 2) \leftarrow (0, 1)	217 105 180.2(9)	Calc.	83
	217 105 181.901(76)	Exp., Doppler	93
	217 105 181.901(50)	Exp., Lamb dip	94
	217 105 182.11(24)	Exp., Lamb dip	95
	217 105 182.285(27)	Exp., Lamb dip	71
	217 105 181.898(20)	Exp., Doppler	92
(2, 0) \leftarrow (0, 1)	209 784 240.1(10)	Calc.	73
	209 784 242.007(20)	Exp., Lamb dip	96
(2, 3) \leftarrow (0, 2)	219 042 854.9(9)	Calc.	83
	219 042 856.621(28)	Exp., Lamb dip	97
(2, 4) \leftarrow (0, 3)	220 704 303.2(9)	Calc.	83
	220 704 304.951(28)	Exp., Lamb dip	97
	220 704 305.23(24)	Exp., Lamb dip	95
$D_0^{N=0}$	1 091 417 901.4(8)	Calc.	62
	1 091 417 937.0(108)	Exp.	98
HT			
(1, 0) \leftarrow (0, 0)	102 973 113.1(130)	Calc.	88
	102 973 087.6(159)	Exp., CARS	88
(1, 1) \leftarrow (0, 1)	102 876 046.3(130)	Calc.	88
	102 876 033.1(159)	Exp., CARS	88
$D_0^{N=0}$	1 094 608 205.6(8)	Calc.	62
DT			
(1, 0) \leftarrow (0, 0)	82 243 316.3(33)	Calc.	99
	82 243 315.4(120)	Exp., CARS	99
(1, 1) \leftarrow (0, 1)	82 195 060.2(33)	Calc.	99
	82 195 054.5(99)	Exp., CARS	99
$D_0^{N=0}$	1 105 672 994.5(8)	Calc.	62

Table 3 Calculated¹⁰¹ coefficients between the $R_2(1)$ transition frequency of HD and the Rydberg constant R_y , the fine structure constant α , the proton mass m_p , the deuteron mass m_d , the electron mass m_e , and the sum of proton and deuteron charge radii squares $r^2 = r_d^2 + r_p^2$. Values of C and uncertainties $\delta C/C$ are taken from CODATA 2018¹⁰²

Constant	Value	$\delta C/C$	β
R_y	109737.315681 60(21) cm ⁻¹	1.9×10^{-12}	1
α^{-1}	137.035999084(21)	1.5×10^{-10}	4.3×10^{-6}
m_p/m_e	1836.15267343(11)	6.0×10^{-11}	-0.314
m_d/m_e	3670.48296788(13)	3.5×10^{-11}	-0.157
r^2	5.2363(63) fm ²	0.0012	-2.9×10^{-9}

uncertainty of 2×10^{-11} , measurement of the transition frequency will lead to a determination of the m_p/m_e value with a precision as same as presented in CODATA 2018.

3. Ro-vibrational spectroscopy

3.1 Doppler-limited spectra

At room temperature, the ro-vibrational transitions of the hydrogen molecule in the infrared are Doppler broadened to

several hundred MHz to a few GHz. The accuracy of the measurement will be mainly limited by the signal-to-noise ratio (SNR) of the spectrum, which can be roughly estimated by dividing the linewidth of the transition by SNR. We have collected the precise transition frequencies of the H₂ and HD molecules in Tables 1 and 2 from the literature. Due to space limitations, only the results with the best accuracy so far are given here.

H₂. In 1938, Herzberg proposed¹⁰³ to use the quadrupole transitions of H₂ to identify the hydrogen content in hydrogen-rich planetary atmospheres. It was not until 1949 that he realized the first measurement of the transitions in the $V = 3 \leftarrow 0$ overtone band near 0.8 μm in laboratory,¹⁰⁴ which is also the first measurement of molecular quadrupole transitions. He used a 22 meter-long sample cell containing hydrogen gas with pressure as high as 10 atm, and an absorption path length of up to 55 km was realized by 250 passes in the cell. In total, 8 lines in the $V = 2 \leftarrow 0$ and $3 \leftarrow 0$ bands were detected with a frequency accuracy of 10^{-2} cm^{-1} .

Since Herzberg's pioneering work, with the development of spectroscopic techniques, especially the application of Fourier-transform (FT) spectroscopy combined with multi-pass absorption cells, spectroscopy of molecular hydrogen has been improved in both accuracy and sensitivity. In the 1980s, Jennings and Brault¹⁰⁵ measured FT spectra of pure rotational transitions of H₂. While in the meantime, Bragg *et al.* presented the results of 22 transitions of H₂ to ro-vibrational states of $V = 1, 2, 3,$ and 4 and reported the line intensities, as well as the line centers and pressure-induced line shifts.¹⁰⁶ Ferguson *et al.* measured the S(1) line in the $V = 5 \leftarrow 0$ band using a dye laser and a White cell,¹⁰⁷ which is the highest overtone transition of H₂ experimentally measured so far.

In recent years, the emergence of highly sensitive cavity-enhanced spectroscopy techniques, such as cavity ring-down spectroscopy (CRDS),¹⁰⁸ has greatly advanced the study of weak molecular transitions. The infrared spectra of molecular hydrogen have been detected under relatively low pressures benefiting from that. Consequently, pressure-induced broadening and shift were reduced, better signal-to-noise ratios were achieved, and the accuracy of transition frequencies has been significantly improved in the last decade. The review of the observations of H₂ absorption lines available in the literature up to 2012 is presented in Table 3 of Campargue.⁶⁷ The first overtone $V = 2 \leftarrow 0$ band of H₂ was measured by the Grenoble group led by Campargue⁶⁷ using CRDS, and the second overtone $V = 3 \leftarrow 0$ band was measured by Robie and Hodges¹⁰⁹ and also by the authors' group at Hefei.^{110,111} Using a highly stable etalon and the rubidium atomic transition as the frequency reference, we have successfully improved the frequency calibration accuracy around 0.8 μm to within 1 MHz,¹¹² and determined the center of the S(3) line in the $V = 3 \leftarrow 0$ band with an accuracy of 1.6 MHz (fractional uncertainty 4×10^{-9}).⁸⁰ It is worth noting that the S₃(5) ($V = 3 \leftarrow 0, J = 7 \leftarrow 5$) transition has a strength of only $9.2 \times 10^{-31} \text{ cm mol}^{-1}$, which is among the weakest transitions observed so far by absorption spectroscopy. For stronger lines in this band, such as S(1), the line strength

derived from experimental data¹¹⁰ agrees to the calculated result⁶⁷ within 2%, while the previous measurement¹⁰⁹ gave a discrepancy as large as 20%.

The collisional effects and their consequences in line profiles are exceptionally sound in the hydrogen molecule due to its large rotational constant and the lack of low-temperature inelastic channels in H₂ scattering, which makes it a perfect subject for testing the collision-induced line shape models.¹¹³ The collision-induced translational velocity changes for Q(1) lines in pure H₂ and H₂-Ar mixtures were presented with both *ab initio* molecular dynamics simulations (MDSS) and the Billiard-ball (BB) model by Wcislo *et al.*¹⁹ The collisional line-shape effects of H₂ lines perturbed by rare gases were investigated by Słowiński *et al.*¹¹⁴ and Thibault *et al.*,¹¹⁵ and compared to *ab initio* calculations.^{20,21}

D₂. For another homonuclear isotopologue D₂, the transition strength is weaker than that of H₂, and fewer infra-red transitions have been reported. In 1978, McKellar and Oka¹¹⁶ measured 11 lines in the $V = 1 \leftarrow 0$ band with a frequency accuracy of 0.004 cm^{-1} using frequency-modulation spectroscopy, and determined rotational constants of the $V = 0, 1$ state of D₂. The $V = 1 \leftarrow 0$ band of D₂ was also investigated by Maddaloni *et al.*¹¹⁷ using CRDS calibrated by an optical comb. The $V = 2 \leftarrow 0$ band of D₂ was measured by CRDS by the Grenoble group.^{66,85,86,118} Frequencies of several lines in this band were recently determined with sub-MHz accuracy.⁸⁵ The S(1) line in the fundamental band of D₂ was measured in a molecular beam by Fast and Meek,⁸⁴ and the transition frequency was determined to be 94 925 100.487(17) MHz, agreeing well with the theoretical result⁷³ of 94 925 100.0(4) MHz.

HD. Because of the mass difference between proton and deuteron, the HD molecule has a weak electric dipole, therefore dipole transitions are allowed among vibration-rotation energy levels of HD.

In 1950, Herzberg first measured 13 electric dipole transitions of HD¹¹⁹ in the vibrational bands of $V = 3 \leftarrow 0$ and $V = 4 \leftarrow 0$, and the transition frequencies were determined with a fractional uncertainty of 7×10^{-8} . Durie and Herzberg measured 23 lines in the bands from the fundamental to the third overtone of HD with the grating spectroscopy.¹²⁰ McKellar and his colleagues^{121,122} derived the centers and intensities of 39 lines with the vibrational quantum number up to 6 from FT spectra. The research group led by Shy from National Tsing Hua University measured the very weak P(5) line in the $V = 2 \leftarrow 0$ band.¹²³ It is worth noting that Drouin *et al.*⁹⁰ measured the pure rotational R(0) line of HD with terahertz spectroscopy, and the relative frequency accuracy reached 10^{-8} .

CRDS measurement of HD transitions was carried out for the fundamental band¹²⁴ at 2.7 μm and the first overtone band^{93,125-127} near 1.4 μm . Not only electric dipole transitions (E1) with selection rules of $\Delta J = \pm 1$, but also quadrupole transitions (E2) of $\Delta J = \pm 2$ lines were measured.¹²⁵

T₂, HT, DT. For a long time, due to the radioactive property of tritium ($t_{1/2} \simeq 12 \text{ y}$), there is a paucity of high-accuracy investigations on the tritium-bearing species of molecular hydrogen. The relativistic and QED effects are completely

unstudied for tritiated isotopologues. Handling tritium-containing samples in a spectroscopy laboratory is restricted to minute amounts, thus ruling out the use of molecular beam techniques, while cavity-enhanced techniques have severe difficulties in material degradation with tritium exposure. Precision tests on T₂, HT, and DT have been performed with coherent anti-Stokes Raman spectroscopy (CARS). The CARS technique offers excellent sensitivity and has been applied to T₂ at 2.5 mbars, which is small enough to avoid the risk of radioactivity. The experimental configuration can be found in ref. 89. As shown in Table 1, the fundamental vibration splitting for $J = 0-5$ rotational levels of T₂ has been determined with an uncertainty of 10–20 MHz, corresponding to a 50-fold improvement over a previous measurement. The result allows for the extraction of relativistic and QED contributions to T₂ transition frequencies. Later in 2020, similar measurements determined the transition frequencies of the fundamental vibrational band of HT and DT with uncertainties below 15 MHz^{88,99} (see Table 2). All measured transition frequencies are in very good agreement with the latest *ab initio* calculations based on NAPT theoretical framework.

3.2 Doppler-free spectroscopy

Precision spectroscopic measurements need to give the transition frequencies of “free” molecules. However, it is difficult to eliminate collisions among gas-phase molecules, which leads to the broadening and shift of the observed spectra. For molecules in thermal equilibrium, the spectra of molecules at different pressures are measured and a linear extrapolation of the obtained frequencies may give the line position at the zero pressure limit. The linearity has been demonstrated for most molecules in the pressure range of 10³–10⁵ Pa. However, when the pressure line shift is much smaller than the Doppler broadening at low pressures, due to the lack of experimental precision, no line profile model has been verified to the accuracy at the 0.1% level of the line width. Therefore, the reliability of this linear extrapolation is questionable. Weislo *et al.* concluded¹⁶ that the presence of nonlinearity at low pressures may induce a deviation of several MHz on the center of the S(3) line in the $V = 3 \leftarrow 0$ band of H₂.

In order to reduce the possible deviation caused by the uncertainty of the spectral line shape, the best method is to reduce or even eliminate the Doppler broadening. The most commonly used method is saturated absorption spectroscopy. The saturation intensity of an infrared transition can be calculated as:¹²⁸

$$I_s = \frac{8\pi^3 hc \Gamma^2}{3A \lambda^3}, \quad (3)$$

where h is the Planck constant, c is the speed of light, λ is the wavelength of the transition, A is the Einstein A-coefficient of the transition, and Γ is the width (FWHM) of the saturated absorption line. For molecules in a static cell, the width Γ mainly comes from the transit-time broadening, the collision broadening, and the natural width. When the measured molecular transition is very weak, the natural width is negligible,

while the transit-time width is around several hundred kHz at room temperature. Therefore, a very strong laser is required to saturate the transition. Taking the R(1) line in the $V = 2 \leftarrow 0$ band of HD near 1.4 μm as an example, the saturation intensity is as high as $3 \times 10^8 \text{ W cm}^{-2}$.

High-finesse cavities used in cavity-enhanced spectroscopy not only enhance the detection sensitivity but also significantly increase the intra-cavity laser power, which is necessary for saturation spectroscopy measurement. Various cavity-enhanced saturated absorption spectroscopy techniques^{128–131} have been employed to measure saturated spectra (Lamb dips) of weak molecular ro-vibrational transitions.

Because of the relatively strong transition dipole and available mature diode lasers in the near-infrared region, lines in the $V = 2 \leftarrow 0$ band of HD are the best candidates for saturated absorption spectroscopy of the hydrogen molecule. Cavity ring-down spectroscopy of Lamb dips of HD was first implemented by the group in Hefei. By using continuous-wave diode lasers of 10 mW and resonant cavity with a finesse of about 1.2×10^5 , an intra-cavity laser power of about 200 W was realized, leading to a saturation parameter of about 0.001 for the R(1) line in the $V = 2 \leftarrow 0$ band. A Lamb “dip” with a depth of about $5 \times 10^{-12} \text{ cm}^{-1}$ and a width of about 0.9 MHz was observed,¹⁰¹ which was fitted by a Lorentzian profile and gave the line center with an uncertainty below 0.1 MHz. To the best of our knowledge, this is also one of the weakest molecular transitions measured by saturated absorption spectroscopy at that moment. The same line was also observed by the Amsterdam group⁹⁷ led by Ubachs using the noise-immune cavity-enhanced optical heterodyne molecular spectroscopy (NICE-OHMS) method.¹³² However, the position given by the Amsterdam group differs from that given by the Hefei group by 0.9 MHz, which is almost 10 times the combined uncertainty of both groups.

Such a big discrepancy has driven considerable efforts to search for potential causes, either technical or physical. Both the Amsterdam and Hefei groups have measured a C₂H₂ line close to the HD line with respectively same methods used to record the HD spectra, and positions of this C₂H₂ line determined by two groups agree within 10 kHz. Later an Italian group at Caserta measured the Doppler-broadened spectrum of the R(1) line and gave the position as 217 105 181 581(94) kHz.¹²⁶ Since the Doppler width of the HD line is about 1 GHz, various interference needs to be considered in the Doppler-broadened measurement, including the influence due to a nearby HDO line which is 410 MHz red-shifted to the HD line. Recently the Italian group remeasured the spectrum and took into account the hyperfine structure^{133–135} in the fitting, and the revised result is given⁹³ as 217 105 181 901(76) kHz. The Campargue’s group⁹² measured the Doppler-limited spectrum of R(1) transition at 80 K and gave the position as 217 105 181 898(33) kHz. Using a molecular beam, Fast *et al.*⁹¹ reported the R(0) line in the $V = 1 \leftarrow 0$ band and conclude an absolute frequency of 111 448 815 477(13) kHz. Saturated spectroscopy of the R(1) line was also remeasured by the Amsterdam group⁹⁴ using the NICE-OHMS method, and they found that the spectrum actually

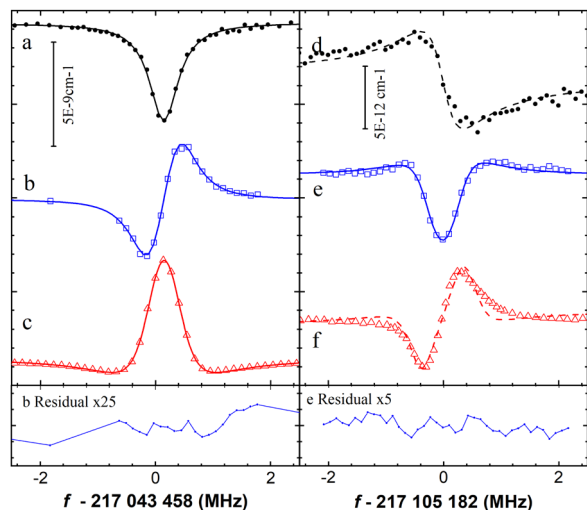


Fig. 1 Saturated absorption spectra of the R(1) $V = 2 \leftarrow 0$ line of HD at 1380.86 nm (right panels) and a nearby C_2H_2 line at 1381.26 nm (left panels). Three different spectroscopy methods were used: CRDS (a) and (d), wavelength-modulated CEAS (b) and (e), and wavelength-modulated NICE-OHMS. [Reprinted/Adapted] with permission from ref. 95 © The Optical Society.

consists of a dip and a peak, which could not be described by a symmetric Lorentzian profile. The Amsterdam group applied a hypothesis of a mechanism refilling the ground state population among the hyperfine sub-levels and gave a revised R(1) position of 217 105 181 901(50) kHz based on numerical simulations.

After improving the experimental sensitivity, the Hefei group also remeasured the Lamb “dip” spectrum of the line using all three different cavity-enhanced spectroscopy, CRDS, NICE-OHMS, and CEAS.^{95,131} All three methods gave consistent results for both the R(1) line of HD and a nearby line of C_2H_2 , and the results are shown in Fig. 1. We can see that the CRDS data of C_2H_2 (Fig. 1a) shows a normal Lamb “dip” feature, while the wavelength-modulated (wm) CEAS spectrum (Fig. 1b) resembles the first derivative of the absorption spectrum, and the wm-NICE-OHMS spectrum (Fig. 1c) gives the second derivative of Fig. 1a. However, the CRDS spectrum of the HD line (Fig. 1d) has a dispersion-like profile, while the wm-CEAS and wm-NICE-OHMS spectra (Fig. 1e and f) remain to be the first and second derivatives of the CRDS spectrum. The result clearly shows that the spectrum of HD is totally different from the normal saturated spectrum of other molecular transitions. The abnormal feature gives the reason for the previous disagreement between the Hefei and Amsterdam results.^{97,101} The latest results of the transitions in the $V = 2 \leftarrow 0$ band of HD are presented in Table 2. We can see a deviation of almost 2 MHz between the experimental and theoretical frequencies, which is roughly twice that for the $V = 1 \leftarrow 0$ band. Although such a systematic shift is insignificant (2σ) compared to the present theoretical uncertainty, it indicates that further investigation is needed to eliminate the discrepancy between the theory and experiments.

The HD gas has a large vapor pressure at low temperatures, and saturated absorption spectra of R(0) and R(1) at sample

temperatures as low as 20 K were measured. The R(1) transition was measured at 76 K and the measured Lamb-dip signal shows an asymmetric line profile, as shown in Fig. 2. The asymmetric line profile in the measurement can be proved by quantum optics theory and described with the Fano model proposed in ref. 136. The line profile is fitted and the line center was measured to be 217 105 182 284(11)_{stat}(27)_{sys} kHz after systematic corrections.⁷¹ Note that Lamb dip measurements reduce the statistical uncertainty but do not exclude systematic errors, which needs carefully treatments. Recently the Lamb dip of a quadrupole transition in H_2 is observed that leads to more interests for understanding the line shape of the Doppler-reduced measurements.¹³⁷

An alternative choice is to measure high overtones, such as the $V = 4 \leftarrow 0$ band of HD, which turns out to be difficult since the transition moment is extremely small. However, it is possible to access the $V = 4$ state with the double resonance method. This method needs to lock the two lasers onto a high-reflectivity cavity and maintain a high intra-cavity power, which is not easy to achieve in experiments. We have demonstrated cavity-enhanced double resonance spectroscopy measurements for CO_2 and CO , and the details can be found in ref. 138 and 139. We obtained a result in HD using the wavelength-modulated cavity-enhanced method because the signal-to-noise ratio is a bit better than CRDS. The V-type double resonance spectrum of P(1) and R(1) was measured and it is shown in ref. 72, where the sum of R(1) and P(1) transition frequencies $\omega_{R1} + \omega_{P1}$ is determined as 426 889 423 917(26) kHz. In the V-type double resonance measurement, complicated photon-molecule interaction leads to possible exists systematic effect, requiring more investigations. If the systematic error is clearly derived or even eliminated and the theoretical calculation reaches the corresponding precision, the vibrational transition measurement will lead to a determination of the fundamental constant such as the proton-to-electron mass ratio with a precision of 11 digits.

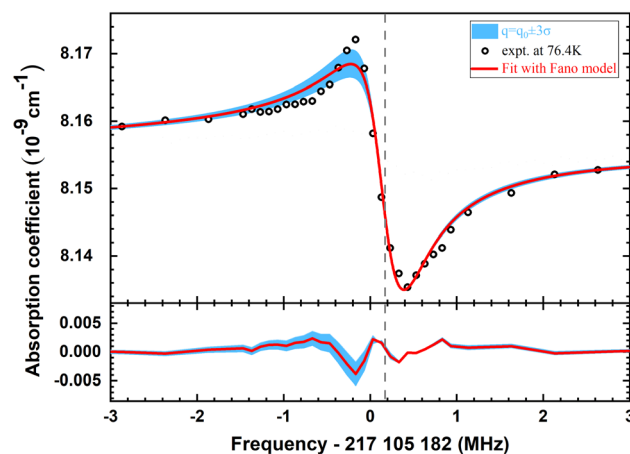


Fig. 2 Saturated absorption spectra of the R(1) $V = 2 \leftarrow 0$ line of HD. Reprinted figure with permission from the ref. 71, Copyright (2023) by the American Physical Society.

4. Precise electronic spectroscopy

The dissociation energy (D_0) of the electronic ground state of the hydrogen molecule, which is the lowest amount of energy that is needed to dissociate the molecule from the ground state into two separate neutral hydrogen atoms in their ground state, is one of the best calculable energy intervals of the hydrogen molecule. More than a century ago, before the development of quantum mechanics, the first experimental determination of $D_0(\text{H}_2)$ was reported by Langmuir.¹⁴⁰ Langmuir's experiment involved heating up H_2 gas, and measuring how much energy was needed to dissociate the molecule. He was measuring power consumption to maintain the wire sensor in the gas at the given temperature. In 1926, Witmer was the first to determine D_0 by determining the vibrational splittings in the ground state of H_2 from measurements of the Lyman bands in a discharge cell.¹⁴¹ In 1927, just after the birth of quantum mechanics, Heitler and London were the first to show that molecular binding is a direct consequence of quantum mechanics and published the first theoretical value of the dissociation energy.¹ This is the first modern explanation of the chemical bond between two neutral atoms and is one of the earliest applications of quantum chemistry theory. Despite their calculated dissociation energy being off by some 30% from the contemporary experimental value, their pioneering quantum mechanical calculation for the stability of molecular hydrogen ushered in the era of quantum chemistry. Theoretical and experimental physicists inspired each other in the following decades to decrease the uncertainty in D_0 , as shown in Fig. 3.

Direct measurement of dissociation energies in H_2 turned out to be difficult. By using a large vacuum spectrograph to study the far UV absorption edges of H_2 , Herzberg determined the second dissociation limit, *i.e.* the energy where dissociation results with one of the atoms in the $n = 1$ state and the other in the $n = 2$ state.²⁷ From this energy, a significantly improved experimental value for D_0 is derived by subtracting the energy

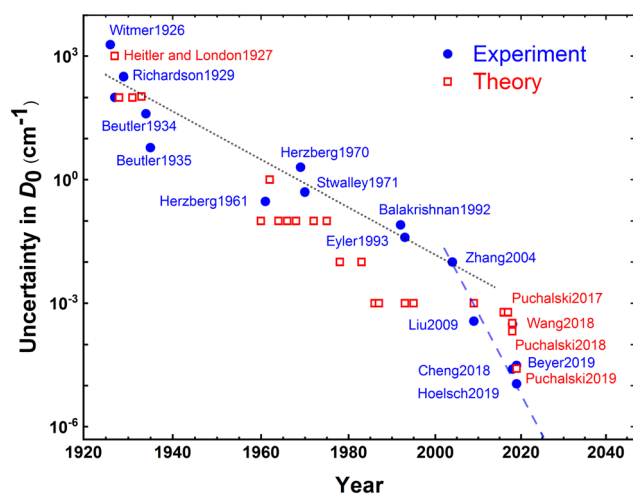


Fig. 3 History of the uncertainty in the dissociation energy of H_2 . The Langmuir's result is not shown.

required to excite the atom to the $n = 2$ state. After the invention of lasers, the accuracy of D_0 was improved dramatically. Eyler *et al.*¹⁴² and Zhang *et al.*¹⁴³ studied the second dissociation limit to determine D_0 using double-resonance laser spectroscopy. All these techniques revolved around getting as close to a dissociation limit as possible. However, since there is no discrete quantum state at the dissociation limit, these methods are fundamentally limited by the accuracy of the D_0 value.

The so-called “thermochemical cycle” was applied to circumvent this problem by Liu *et al.*^{68,144} for H_2 and D_2 and Sprecher *et al.*⁹⁸ for HD. As shown in Fig. 4, the D_0 value could be determined from the ionization energies of the neutral molecule $E_i(\text{H}_2)$, the molecular ion $E_i(\text{H}_2^+)$, and the atom $E_i(\text{H})$. According to this thermochemical cycle, we have:

$$D_0(\text{H}_2) = E_i(\text{H}_2) + E_i(\text{H}_2^+) - 2 \times E_i(\text{H}),$$

and similarly for HD:

$$D_0(\text{HD}) = E_i(\text{HD}) + E_i(\text{HD}^+) - E_i(\text{H}) - E_i(\text{D}).$$

Following the equations, the dissociation energies can be determined if we know the ionization energies of the atoms and molecular ions. Since the H and D atoms and the H_2^+ , D_2^+ , and HD^+ molecular ions are single-electron systems simpler than respective neutral molecules, their ionization energies could be calculated with a better precision.^{145,146} The calculated energies of these single-electron systems have been tested to the kHz accuracy.^{147,148} Ionization energies of H and D atoms have been experimentally determined with an accuracy of 3 kHz.¹⁴⁶ Ionization energies of the H_2^+ , D_2^+ , and HD^+ molecular ions are known with an accuracy of 18 kHz.¹⁴⁵ Therefore, the accuracy of the dissociation energies currently

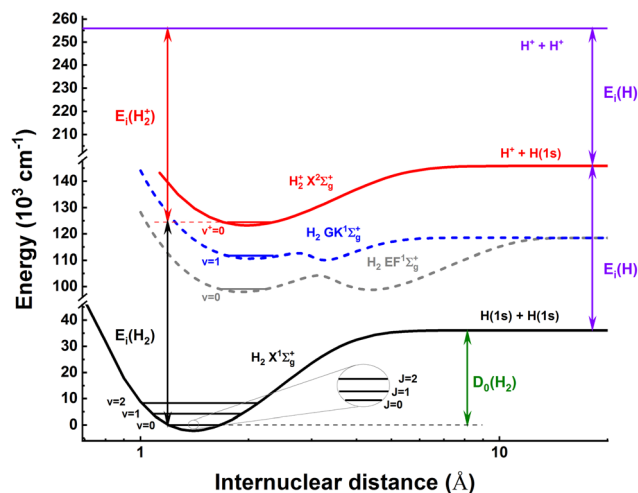


Fig. 4 Potential energy diagrams of the $X^1\Sigma_g^+$, $EF^1\Sigma_g^+$, and $GK^1\Sigma_g^+$ states in H_2 and the $X^2\Sigma_g^+$ in H_2^+ . Horizontal lines indicate the lowest three vibrational levels and the lowest three rotational levels in the $v = 0$ level of the $X^1\Sigma_g^+$ state of H_2 , the first vibrational level of the inner well of the $EF^1\Sigma_g^+$ state and that of the $GK^1\Sigma_g^+$ state of H_2 , and the first vibrational level of the $X^2\Sigma_g^+$ state of H_2^+ . Arrows illustrate how the D_0 value of H_2 can be obtained from $E_i(\text{H}_2)$, $E_i(\text{H}_2^+)$ and $E_i(\text{H})$.

depends on the accuracy of the ionization energies of the neutral molecules.

Liu *et al.*⁶⁸ determined the ionization energy of the H₂ molecule at a relative accuracy of 10⁻⁹, involving two-photon laser excitation to the EF¹Σ_g⁺ (V = 0, N = 1) intermediate state,¹⁴⁹ one-photon ultraviolet excitation from EF¹Σ_g⁺ (0, 1) to the 56p₁ Rydberg state,⁶⁸ and millimeter-wave (MMW) spectroscopy of high-lying Rydberg states¹⁵⁰ allowing for an extrapolation to the ionization energy by the Multi-Channel Quantum Defect theory (MQDT).¹⁵¹ The first measurement on high-lying Rydberg states to extrapolate the ionization potential was carried out by Herzberg and Jungen²⁸ in 1972. Since the Rydberg series have infinite states with increasing principal quantum number *n*, it is reasonable to converge to the ionization limit and there is no fundamental limit to how close a state can be. However, the Rydberg electron interacts with the vibrational and rotational modes of the H₂⁺ core. This heavily perturbs the Rydberg states. The method of MQDT, by which the ionization limit of a (measured) Rydberg series can be extrapolated, was extended to molecules to account for these perturbations,^{28,152} which is the principle limitation of this method and the thermochemical cycle. In this way, the accuracy of the determinations of the dissociation energy of the neutral molecules by the Zürich-Amsterdam collaboration was improved to 11 MHz for H₂ and HD, and to 20 MHz for D₂.^{98,144,153}

In 2018, an alternative excitation scheme was adopted to determine D₀(H₂) through the GK¹Σ_g⁺ (1,1) intermediate state as shown in Fig. 4, which offers the possibility of using continuous-wave (CW) infrared laser excitation to high-*n* Rydberg states.¹⁵⁴ Experimental results from two laboratories are combined: the measurement of the Doppler-free two-photon transition GK(1,1) ← X(0, 1) in Amsterdam, and the determination of the interval between GK(1,1) and the 56p₁ Rydberg state by near-infrared (NIR) CW-laser spectroscopy in Zürich. The accuracy of D₀^{N=1}(H₂) was then improved to 0.75 MHz.⁸² Similar method was used for D₀^{N=0}(H₂)⁸¹ and D₀^{N=0}(D₂)¹⁵⁵ with uncertainties of 0.78 MHz and 0.97 MHz, respectively. The former result, compared with D₀^{N=1}(H₂), was used to test the nuclear-spin-symmetry conservation in molecular hydrogen.⁸¹ A new technology of Ramsey-comb method¹⁵⁶ has been applied to improve the dissociation energy D₀^{N=1} of H₂ and the accuracy reached 0.34 MHz,⁷⁴ which is so far the best dissociation energy measurement.

The non-zero nuclear spin in the molecular hydrogen system, the vector of which is denote as \vec{I} , leads to a hyperfine splitting for low-lying rotational state from a few kHz to hundreds of kHz, which is considered as a part of the uncertainty contribution in the transition measurement. Because the electronic transitions of the neutral hydrogen molecule can be determined to an accuracy at the MHz level, the rotationless fundamental ground tone, *i.e.*, the vibrational energy splitting between the (V = 1, J = 0) and (V = 0, J = 0) states, is possible to be determined to the similar accuracy utilizing the differences between electronic transitions. The rotationless fundamental ground tone is an ideal test system for several reasons. The total electronic angular momentum is zero for the X¹Σ_g⁺ ground state

and the total nuclear spin for the rotationless J = 0 state of *para*-H₂ is also zero resulting in a simple spectrum without hyperfine splitting. The hyperfine splitting is extremely small in HD (or D₂) in the absence of an $\vec{I}\vec{J}$ interaction for the J = 0 ground state. Energy contributions in the calculation almost cancel the fundamental ground tone, leading to a significant reduction in the uncertainty, thereby allowing for accurate QED tests. However, in the absence of rotation, a one-photon transition between the (V = 1, J = 0) and (V = 0, J = 0) states is strictly forbidden by nonrelativistic quantum mechanics. It is the nuclear spin-rotation coupling that makes this transition possible for D₂ and HD, but the oscillator strength is extremely small, and it remains zero for H₂. Therefore, an experimental approach is adopted to measure this quantity *via* the combination difference of separate two-photon transitions involving a common electronically excited state (EF¹Σ_g⁺, V = 0, J = 0) has been performed.¹⁵⁷ The rotationless fundamental ground tone frequencies of H₂, HD and D₂ were determined to 4164.166 32(18) cm⁻¹, 3632.160 54(24) cm⁻¹ and 2993.617 13(17) cm⁻¹, respectively. The results could be improved by another factor of ten if the Ramsey-comb technique¹⁵⁶ is used.

5. Conclusion and perspective

The hydrogen molecule is a four-body system consisting of two electrons and two nuclei. Its energy levels can be calculated with high precision based on quantum electrodynamics and a few fundamental physical constants without using any adjustable parameters. The comparison between theoretical calculations and precision spectroscopy experiments can test theories and determine fundamental physical constants. The accuracy of theoretical and experimental measurements of the hydrogen molecule, especially in its electronic ground state, has been continuously improved in the last 80 years. So far the quantum electrodynamics correction to the energies of the hydrogen molecule has been evaluated and the accuracy reaches the level of 1 MHz for the dissociation energy, agreeing well with the most recent measurements in H₂ and D₂. Further investigation of the high-order nonadiabatic E⁽⁷⁾, E⁽⁸⁾ energy terms will make molecular hydrogen a cornerstone in quantum mechanics, which has not yet been accomplished for any other systems except the hydrogen atom and molecular hydrogen ion.

Doppler-broadened infrared laser spectroscopy of molecular hydrogen has reached a fractional accuracy of 10⁻⁹, but further improvement is limited by the broad linewidth and the presence of collision-induced shifts. Understanding the line-shape model needs massive work, both in experiments and *ab initio* calculations.¹⁵⁸ Measurements based on the Doppler-free saturated absorption spectroscopy are currently only possible for relatively strong electronic dipole transitions of the HD molecule. However, the asymmetric line profile complicates the determination of the center frequency toward the 10⁻¹⁰ accuracy. Using the Ramsey-comb technique, the electronic transition of EF-X has been improved to an accuracy of 73 kHz, which represents the best measurement of electronic transitions of

molecular hydrogen. This advanced technology provides new opportunities to reach more accurate dissociation energy and requires higher precision measurement of the energy interval between the EF state and molecular hydrogen ion. The latter difficulty is even more pronounced in the HD molecule due to the mixing of Rydberg states of *g* and *u* symmetry through the dipole of the HD⁺ core arising from the separation of the center of mass from the center of charge.^{70,159}

Besides precise energies of molecular hydrogen, other microscopic properties of the hydrogen molecule, such as transition strengths among the vibrational states and static polarizabilities of low-lying states, are also possible test grounds for high-precision calculations. The transition moments are useful for understanding wavefunctions of the molecule. Polarizabilities are related to many physical quantities, such as the refractive index, dielectric constant, and van der Waals constant. As an example, accurate theoretical polarizability of the molecular hydrogen allows for primary pressure standard based on the measurement of refractive index.

Regarding the possibility of determination of the fundamental physical constants, an outstanding target in the spotlight is the proton charge radius. In atomic hydrogen, there is no other narrow transition except the 1s–2s transition, and the present determination based on the electronic hydrogen atom (e-H) relies on an average of many transitions with much larger natural linewidth. The neutral hydrogen molecule has more than 300 ro-vibrational states with lifetimes of several days. In principle, these transitions could be measured with 20-digit accuracy.¹⁶⁰ Precision spectroscopy of different isotopologues of the hydrogen molecule, and comparison to different substitutions of e-H, such as the muonic hydrogen (μ -H) and anti-hydrogen (\bar{H}), could be used to test the violation of lepton universality and search for new physics beyond the Standard Model.

Author contributions

Qian-Hao Liu: data curation, visualization, and writing – original draft; Yan Tan: writing – original draft and writing – review & editing; Cun-Feng Cheng: project administration, writing – original draft and writing – review & editing; Shui-Ming Hu: supervision, writing – original draft and writing – review & editing.

Conflicts of interest

There are no conflicts to declare.

Acknowledgements

This work was jointly supported by Chinese Academy of Science (grant no. YSBR-055, XDC07010000), Ministry of Science and Technology of China (grant no. 2022YFF0606500, 2021ZD0303102), and National Natural Science Foundation of China (grant no. 11974328, 22241302).

Notes and references

- W. Heitler and F. London, *Z. Phys.*, 1927, **44**, 455–472.
- K. Pachucki and J. Komasa, *J. Chem. Phys.*, 2016, **144**, 164306.
- M. Puchalski, J. Komasa, P. Czachorowski and K. Pachucki, *Phys. Rev. Lett.*, 2016, **117**, 263002.
- E. J. Salumbides, G. D. Dickenson, T. I. Ivanov and W. Ubachs, *Phys. Rev. Lett.*, 2011, **107**, 043005.
- M. Puchalski, J. Komasa and K. Pachucki, *Phys. Rev. A*, 2017, **95**, 052506.
- W. Ubachs, J. C. J. Koelemeij, K. S. E. Eikema and E. J. Salumbides, *J. Mol. Spectrosc.*, 2016, **320**, 1–12.
- E. J. Salumbides, J. C. J. Koelemeij, J. Komasa, K. Pachucki, K. S. E. Eikema and W. Ubachs, *Phys. Rev. D*, 2013, **87**, 112008.
- W. Vassen, *Science*, 2017, **358**, 39–40.
- E. Roueff, H. Abgrall, P. Czachorowski, K. Pachucki, M. Puchalski and J. Komasa, *Astron. Astrophys.*, 2019, **630**, A58.
- Y. Tan, F. M. Skinner, S. Samuels, R. J. Hargreaves, R. Hashemi and I. E. Gordon, *Astrophys. J., Suppl. Ser.*, 2022, **262**, 40.
- J. M. Hartmann, H. Tran, R. Armante, C. Boulet, A. Campargue, F. Forget, L. Gianfrani, I. Gordon, S. Guerlet, M. Gustafsson, J. T. Hodges, S. Kassı, D. Lisak, F. Thibault and G. C. Toon, *J. Quant. Spectrosc. Radiat. Transf.*, 2018, **213**, 178–227.
- T. Owen, *Science*, 1970, **167**, 1675–1681.
- J. S. Margolis and G. E. Hunt, *Icarus*, 1973, **18**, 593–598.
- J. Tennyson, P. F. Bernath, A. Campargue, A. G. Császár, L. Daumont, R. R. Gamache, J. T. Hodges, D. Lisak, O. V. Naumenko, L. S. Rothman, H. Tran, N. F. Zobov, J. Buldyreva, C. D. Boone, M. D. D. Vizia, L. Gianfrani, J.-M. Hartmann, R. McPheat, D. Weidmann, J. Murray, N. H. Ngo and O. L. Polyansky, *Pure Appl. Chem.*, 2014, **86**, 1931–1943.
- I. E. Gordon, L. S. Rothman, R. J. Hargreaves, R. Hashemi, E. V. Karlovets, F. M. Skinner, E. K. Conway, C. Hill, R. V. Kochanov, Y. Tan, P. Weislo, A. A. Finenko, K. Nelson, P. F. Bernath, M. Birk, V. Boudon, A. Campargue, K. V. Chance, A. Coustenis, B. J. Drouin, J. M. Flaud, R. R. Gamache, J. T. Hodges, D. Jacquemart, E. J. Mlawer, A. V. Nikitin, V. I. Perevalov, M. Rotger, J. Tennyson, G. C. Toon, H. Tran, V. G. Tyuterev, E. M. Adkins, A. Baker, A. Barbe, E. Canè, A. G. Császár, A. Dudaryonok, O. Egorov, A. J. Fleisher, H. Fleurbaey, A. Foltynowicz, T. Furtenbacher, J. J. Harrison, J. M. Hartmann, V. M. Horneman, X. Huang, T. Karman, J. Karns, S. Kassı, I. Kleiner, V. Kofman, F. Kwabia-Tchana, N. N. Lavrentieva, T. J. Lee, D. A. Long, A. A. Lukashchinskaya, O. M. Lyulin, V. Y. Makhnev, W. Matt, S. T. Massie, M. Melosso, S. N. Mikhailenko, D. Mondelain, H. S. P. Müller, O. V. Naumenko, A. Perrin, O. L. Polyansky, E. Raddaoui, P. L. Raston, Z. D. Reed, M. Rey, C. Richard, R. Tóbiás, I. Sadiék, D. W. Schwenke, E. Starikova, K. Sung, F. Tamassia, S. A. Tashkun, J. Vander

- Auwera, I. A. Vasilenko, A. A. Vigin, G. L. Villanueva, B. Vispoel, G. Wagner, A. Yachmenev and S. N. Yurchenko, *J. Quant. Spectrosc. Radiat. Transfer*, 2022, **277**, 107949.
- 16 P. Wcisło, I. E. Gordon, C.-F. Cheng, S.-M. Hu and R. Ciuryło, *Phys. Rev. A*, 2016, **93**, 022501.
- 17 M. De Vizia, A. Castrillo, E. Fasci, P. Amodio, L. Moretti and L. Gianfrani, *Phys. Rev. A*, 2014, **90**, 022503.
- 18 H. Tran, J.-M. Hartmann, F. Chaussard and M. Gupta, *J. Chem. Phys.*, 2009, **131**, 154303.
- 19 P. Wcisło, H. Tran, S. Kassı, A. Campargue, F. Thibault and R. Ciuryło, *J. Chem. Phys.*, 2014, **141**, 074301.
- 20 M. Słowiński, F. Thibault, Y. Tan, J. Wang, A.-W. Liu, S.-M. Hu, S. Kassı, A. Campargue, M. Konefał, H. Jóźwiak, K. Patkowski, P. Żuchowski, R. Ciuryło, D. Lisak and P. Wcisło, *Phys. Rev. A*, 2020, **101**, 052705.
- 21 N. Stolarczyk, G. Kowzan, F. Thibault, H. Cybulski, M. Słowiński, Y. Tan, J. Wang, A.-W. Liu, S.-M. Hu and P. Wcisło, *J. Chem. Phys.*, 2023, **158**, 094303.
- 22 H. M. James and A. S. Coolidge, *J. Chem. Phys.*, 1933, **1**, 825–835.
- 23 H. M. James and A. S. Coolidge, *J. Chem. Phys.*, 1935, **3**, 129–130.
- 24 W. Kołos and L. Wolniewicz, *J. Chem. Phys.*, 1964, **41**, 3663–3673.
- 25 W. Kołos and L. Wolniewicz, *J. Chem. Phys.*, 1968, **49**, 404–410.
- 26 W. Kołos and L. Wolniewicz, *Phys. Rev. Lett.*, 1968, **20**, 243–244.
- 27 G. Herzberg and A. Monfils, *J. Mol. Spectrosc.*, 1961, **5**, 482–498.
- 28 G. Herzberg, *J. Mol. Spectrosc.*, 1970, **33**, 147–168.
- 29 W. C. Stwalley, *Chem. Phys. Lett.*, 1970, **6**, 241–244.
- 30 W. Kołos and L. Wolniewicz, *J. Mol. Spectrosc.*, 1975, **54**, 303–311.
- 31 W. Kołos, *J. Mol. Spectrosc.*, 1976, **62**, 429–441.
- 32 W. Kołos and J. Rychlewski, *J. Mol. Spectrosc.*, 1976, **62**, 109.
- 33 W. Kołos, K. Szalewicz and H. Monkhorst, *J. Chem. Phys.*, 1986, **84**, 3278–3283.
- 34 L. Wolniewicz and K. Dressler, *J. Mol. Spectrosc.*, 1977, **67**, 416.
- 35 L. Wolniewicz, *J. Chem. Phys.*, 1983, **78**, 6173–6181.
- 36 L. Wolniewicz and K. Dressler, *JCP*, 1985, **82**, 3292.
- 37 L. Wolniewicz and J. Hinze, *J. Chem. Phys.*, 1986, **85**, 2012–2018.
- 38 L. Wolniewicz and J. Poll, *Mol. Phys.*, 1986, **59**, 953–964.
- 39 L. Wolniewicz and K. Dressler, *J. Chem. Phys.*, 1988, **88**, 3861.
- 40 L. Wolniewicz and T. Orlikowski, *Mol. Phys.*, 1991, **74**, 103–111.
- 41 L. Wolniewicz, *J. Chem. Phys.*, 1993, **99**, 1851–1868.
- 42 L. Wolniewicz and K. Dressler, *J. Chem. Phys.*, 1994, **100**, 444.
- 43 L. Wolniewicz, *J. Chem. Phys.*, 1995, **103**, 1792–1799.
- 44 L. Wolniewicz, I. Simbotin and A. Dalgarno, *Astrophys. J., Suppl. Ser.*, 1998, **115**, 293–313.
- 45 L. Wolniewicz, *J. Chem. Phys.*, 1998, **109**, 2254.
- 46 L. Wolniewicz and G. Staszewska, *J. Mol. Spectrosc.*, 2003, **220**, 45–51.
- 47 L. Wolniewicz and G. Staszewska, *J. Mol. Spectr.*, 2003, **217**, 181–185.
- 48 L. Wolniewicz, T. Orlikowski and G. Staszewska, *J. Mol. Spectrosc.*, 2006, **238**, 118.
- 49 W. Kołos and J. Rychlewski, *J. Chem. Phys.*, 1993, **98**, 3960–3967.
- 50 K. Pachucki and J. Komasa, *Phys. Rev. A*, 2008, **78**, 052503.
- 51 K. Pachucki and J. Komasa, *J. Chem. Phys.*, 2009, **130**, 164113.
- 52 K. Pachucki and J. Komasa, *Phys. Chem. Chem. Phys.*, 2010, **12**, 9188–9196.
- 53 K. Pachucki, *Phys. Rev. A*, 2010, **82**, 032509.
- 54 K. Pachucki and J. Komasa, *Phys. Rev. A*, 2011, **83**, 042510.
- 55 K. Pachucki and J. Komasa, *J. Chem. Phys.*, 2014, **141**, 224103.
- 56 K. Pachucki and J. Komasa, *J. Chem. Phys.*, 2015, **143**, 034111.
- 57 K. Pachucki and J. Komasa, *Phys. Chem. Chem. Phys.*, 2018, **20**, 247–255.
- 58 K. Pachucki and J. Komasa, *Phys. Chem. Chem. Phys.*, 2018, **20**, 26297–26302.
- 59 M. Puchalski, J. Komasa, P. Czachorowski and K. Pachucki, *Phys. Rev. Lett.*, 2019, **122**, 103003.
- 60 K. Pachucki and J. Komasa, *Phys. Chem. Chem. Phys.*, 2019, **21**, 10272–10276.
- 61 M. Puchalski, A. Spyszkievicz, J. Komasa and K. Pachucki, *Phys. Rev. Lett.*, 2018, **121**, 073001.
- 62 M. Puchalski, J. Komasa, A. Spyszkievicz and K. Pachucki, *Phys. Rev. A*, 2019, **100**, 020503.
- 63 K. Piszczatowski, G. ach, M. Przybytek, J. Komasa, K. Pachucki and B. Jeziorski, *J. Chem. Theo. Comput.*, 2009, **5**, 3039–3048.
- 64 M. Siłkowski, M. Zientkiewicz and K. Pachucki, *Adv. Quant. Chem.*, 2021, **83**, 255–267.
- 65 M. Siłkowski and K. Pachucki, *Mol. Phys.*, 2022, e2062471.
- 66 S. Kassı, A. Campargue, K. Pachucki and J. Komasa, *J. Chem. Phys.*, 2012, **136**, 184309.
- 67 A. Campargue, S. Kassı, K. Pachucki and J. Komasa, *Phys. Chem. Chem. Phys.*, 2012, **14**, 802–815.
- 68 J. Liu, E. J. Salumbides, U. Hollenstein, J. C. J. Koelemeij, K. S. E. Eikema, W. Ubachs and F. Merkt, *J. Chem. Phys.*, 2009, **130**, 174306.
- 69 L. M. Wang and Z.-C. Yan, *Phys. Rev. A*, 2018, **97**, 060501(R).
- 70 N. Hölsch, I. Doran, F. Merkt, J. Hussels, C.-F. Cheng, E. J. Salumbides, H. L. Bethlem, K. S. E. Eikema, M. Beyer, W. Ubachs and C. Jungen, *Phys. Rev. A*, 2023, **108**, 022811.
- 71 Q.-H. Liu, Y.-N. Lv, C.-L. Zou, C.-F. Cheng and S.-M. Hu, *Phys. Rev. A*, 2022, **106**, 062805.
- 72 M. Y. Yu, Q. H. Liu, C. F. Cheng and S. M. Hu, *Mol. Phys.*, 2022, e2127382.
- 73 J. Komasa, M. Puchalski, P. Czachorowski, G. Lach and K. Pachucki, *Phys. Rev. A*, 2019, **100**, 032519.
- 74 N. Hölsch, M. Beyer, E. J. Salumbides, K. S. E. Eikema, W. Ubachs, Ch Jungen and F. Merkt, *Phys. Rev. Lett.*, 2019, **122**, 103002.

- 75 D. E. Jennings, S. L. Bragg and J. W. Brault, *Astrophys. J. Lett.*, 1984, **282**, L85–L88.
- 76 M. L. Niu, E. J. Salumbides, G. D. Dickenson, K. S. E. Eikema and W. Ubachs, *J. Mol. Spectrosc.*, 2014, **300**, 44–54.
- 77 P. Czachorowski, H2SPECTRE version 7.3, Fortran source code, 2020, <https://qcg.home.amu.edu.pl/H2Spectre.html>.
- 78 M. Lamperti, L. Rutkowski, D. Ronchetti, D. Gatti, R. Gotti, G. Cerullo, F. Thibault, H. Jóźwiak, S. Wójtewicz and P. Masłowski, *et al.*, *Commun. Phys.*, 2023, **6**, 67.
- 79 H. Fleurbaey, A. Koroleva, S. Kassi and A. Campargue, *Phys. Chem. Chem. Phys.*, 2023, **25**, 14749–14756.
- 80 C.-F. Cheng, Y. R. Sun, H. Pan, J. Wang, A. W. Liu, A. Campargue and S.-M. Hu, *Phys. Rev. A*, 2012, **85**, 024501.
- 81 M. Beyer, N. Hölsch, J. Hussels, C.-F. Cheng, E. J. Salumbides, K. S. E. Eikema, W. Ubachs, Ch Jungen and F. Merkt, *Phys. Rev. Lett.*, 2019, **123**, 163002.
- 82 C.-F. Cheng, J. Hussels, M. Niu, H. L. Bethlem, K. S. E. Eikema, E. J. Salumbides, W. Ubachs, M. Beyer, N. Hölsch, J. A. Agner, F. Merkt, L.-G. Tao, S.-M. Hu and C. Jungen, *Phys. Rev. Lett.*, 2018, **121**, 013001.
- 83 P. Czachorowski, M. Puchalski, J. Komasa and K. Pachucki, *Phys. Rev. A*, 2018, **98**, 052506.
- 84 A. Fast and S. A. Meek, *Mol. Phys.*, 2021, e1999520.
- 85 D. Mondelain, S. Kassi and A. Campargue, *J. Quant. Spectrosc. Radiat. Transf.*, 2020, **253**, 107020.
- 86 P. Wcisło, F. Thibault, M. Zaborowski, S. Wójtewicz, A. Cygan, G. Kowzan, P. Masłowski, J. Komasa, M. Puchalski, K. Pachucki, R. Ciuryło and D. Lisak, *J. Quant. Spectrosc. Radiat. Transf.*, 2018, **213**, 41–51.
- 87 J. Hussels, N. Hölsch, C.-F. Cheng, E. J. Salumbides, H. L. Bethlem, K. S. E. Eikema, Ch Jungen, M. Beyer, F. Merkt and W. Ubachs, *Phys. Rev. A*, 2022, **105**, 022820.
- 88 K.-F. Lai, V. Hermann, T. M. Trivikram, M. Diouf, M. Schlösser, W. Ubachs and E. J. Salumbides, *Phys. Chem. Chem. Phys.*, 2020, **22**, 8973–8987.
- 89 T. M. Trivikram, M. Schlösser, W. Ubachs and E. J. Salumbides, *Phys. Rev. Lett.*, 2018, **120**, 163002.
- 90 B. J. Drouin, S. Yu, J. C. Pearson and H. Gupta, *J. Mol. Spectrosc.*, 2011, **1006**, 2–12.
- 91 A. Fast and S. A. Meek, *Phys. Rev. Lett.*, 2020, **125**, 023001.
- 92 S. Kassi, C. Lauzin, J. Chaillot and A. Campargue, *Phys. Chem. Chem. Phys.*, 2022, **24**, 23164.
- 93 A. Castrillo, E. Fasci and L. Gianfrani, *Phys. Rev. A*, 2021, **103**, 022828.
- 94 M. L. Diouf, F. M. J. Cozijn, B. Darquié, E. J. Salumbides and W. Ubachs, *Opt. Lett.*, 2019, **44**, 4733.
- 95 T.-P. Hua, Y. R. Sun and S.-M. Hu, *Opt. Lett.*, 2020, **45**, 4863.
- 96 M. L. Diouf, F. M. J. Cozijn, K.-F. Lai, E. J. Salumbides and W. Ubachs, *Phys. Rev. Res.*, 2020, **2**, 023209.
- 97 F. M. J. Cozijn, P. Dupré, E. J. Salumbides, K. S. E. Eikema and W. Ubachs, *Phys. Rev. Lett.*, 2018, **120**, 153002.
- 98 D. Sprecher, J. Liu, C. Jungen, W. Ubachs and F. Merkt, *J. Chem. Phys.*, 2010, **133**, 111102.
- 99 K.-F. Lai, P. Czachorowski, M. Schlösser, M. Puchalski, J. Komasa, K. Pachucki, W. Ubachs and E. J. Salumbides, *Phys. Rev. Res.*, 2019, **1**, 033124.
- 100 J. Komasa, K. Piszczatowski, G. ach, M. Przybytek, B. Jeziorski and K. Pachucki, *J. Chem. Theo. Comput.*, 2011, **7**, 3105–3115.
- 101 L. G. Tao, A. W. Liu, K. Pachucki, J. Komasa, Y. R. Sun, J. Wang and S. M. Hu, *Phys. Rev. Lett.*, 2018, **120**, 153001.
- 102 E. Tiesinga, P. J. Mohr, D. B. Newell and B. N. Taylor, *J. Phys. Chem. Ref. Data*, 2021, **50**, 033105.
- 103 G. Herzberg, *Astrophys. J.*, 1938, **87**, 428–437.
- 104 G. Herzberg, *Nature*, 1949, **163**, 170.
- 105 D. E. Jennings and J. W. Brault, *J. Mol. Spectrosc.*, 1983, **102**, 265–272.
- 106 S. L. Bragg, J. W. Brault and W. H. Smith, *Astrophys. J.*, 1982, **263**, 999–1004.
- 107 D. W. Ferguson, K. N. Rao, M. E. Mickelson and L. E. Larson, *J. Mol. Spectrosc.*, 1993, **160**, 315–325.
- 108 A. O’Keefe and D. A. G. Deacon, *Rev. Sci. Instrum.*, 1988, **59**, 2544–2551.
- 109 D. C. Robie and J. T. Hodges, *J. Chem. Phys.*, 2006, **124**, 024307.
- 110 S.-M. Hu, H. Pan, C.-F. Cheng, Y. R. Sun, X.-F. Li, J. Wang, A. Campargue and A.-W. Liu, *Astrophys. J.*, 2012, **749**, 76.
- 111 Y. Tan, J. Wang, C.-F. Cheng, X.-Q. Zhao, A.-W. Liu and S.-M. Hu, *J. Mol. Spectrosc.*, 2014, **300**, 60–64.
- 112 C.-F. Cheng, Y. R. Sun, H. Pan, Y. Lu, X.-F. Li, J. Wang, A.-W. Liu and S.-M. Hu, *Opt. Expr.*, 2012, **20**, 9956–9963.
- 113 F. Thibault, R. Z. Martnez, D. Bermejo and P. Wcisło, *Molecular Astrophysics*, 2020, **19**, 100063.
- 114 M. Słowiński, H. Jóźwiak, M. Gancewski, K. Stankiewicz, N. Stolarczyk, Y. Tan, J. Wang, A.-W. Liu, S.-M. Hu and S. Kassi, *et al.*, *J. Quant. Spectrosc. Radiat. Transf.*, 2022, **277**, 107951.
- 115 F. Thibault, K. Patkowski, P. S. Żuchowski, H. Jóźwiak, R. Ciuryło and P. Wcisło, *J. Quant. Spectrosc. Radiat. Transf.*, 2017, **202**, 308–320.
- 116 A. R. W. Mckellar and T. Oka, *Can. J. Phys.*, 1978, **56**, 1315–1320.
- 117 P. Maddaloni, P. Malara, E. De Tommasi, M. De Rosa, I. Ricciardi, G. Gagliardi, F. Tamassia, G. Di Lonardo and P. De Natale, *J. Chem. Phys.*, 2010, **133**, 154317.
- 118 D. Mondelain, S. Kassi, T. Sala, D. Romanini, D. Gatti and A. Campargue, *J. Mol. Spectrosc.*, 2016, **326**, 5–8.
- 119 G. Herzberg, *Nature*, 1950, **166**, 563.
- 120 R. A. Durie and G. Herzberg, *Can. J. Phys.*, 1960, **38**, 806.
- 121 A. R. McKellar, *Can. J. Phys.*, 1974, **52**, 1144–1151.
- 122 A. R. W. McKellar, W. Goetz and D. A. Ramsay, *Astrophys. J.*, 1976, **207**, 663.
- 123 T. Lin, C.-C. Chou, D.-J. Lwo and J.-T. Shy, *Phys. Rev. A*, 2000, **61**, 064502.
- 124 S. Vasilchenko, D. Mondelain, S. Kassi, P. Čermák, B. Chomet, A. Garnache, S. Denet, V. Lecocq and A. Campargue, *J. Mol. Spectrosc.*, 2016, **326**, 9–16.
- 125 S. Kassi and A. Campargue, *J. Mol. Spectrosc.*, 2011, **267**, 36–42.
- 126 E. Fasci, A. Castrillo, H. Dinesan, S. Gravina, L. Moretti and L. Gianfrani, *Phys. Rev. A*, 2018, **98**, 22516.
- 127 S. Kassi, C. Lauzin, J. Chaillot and A. Campargue, *Phys. Chem. Chem. Phys.*, 2022, **24**, 23164–23172.

- 128 G. Giusfredi, S. Bartalini, S. Borri, P. Cancio, I. Galli, D. Mazzotti and P. De Natale, *Phys. Rev. Lett.*, 2010, **104**, 110801.
- 129 D. Gatti, R. Gotti, A. Gambetta, M. Belmonte, G. Galzerano, P. Laporta and M. Marangoni, *Sci. Rep.*, 2016, **6**, 1–8.
- 130 J. Wang, Y. R. Sun, L.-G. Tao, A.-W. Liu, T.-P. Hua, F. Meng and S.-M. Hu, *Rev. Sci. Instrum.*, 2017, **88**, 043108.
- 131 T.-P. Hua, Y. R. Sun, J. Wang, C.-L. Hu, L.-G. Tao, A.-W. Liu and S.-M. Hu, *Chin. J. Chem. Phys.*, 2019, **32**, 107–112.
- 132 J. Ye, L.-S. Ma and J. L. Hall, *J. Opt. Soc. Am. B*, 1998, **15**, 6–15.
- 133 P. Dupré, *Phys. Rev. A*, 2020, **101**, 022504.
- 134 M. Puchalski, J. Komasa and K. Pachucki, *Phys. Rev. Lett.*, 2020, **125**, 253001.
- 135 H. Jóźwiak, H. Cybulski and P. Wcisło, *J. Quant. Spectrosc. Radiat. Transf.*, 2020, **253**, 107171.
- 136 Y.-N. Lv, A.-W. Liu, Y. Tan, C.-L. Hu, T.-P. Hua, X.-B. Zou, Y. R. Sun, C.-L. Zou, G.-C. Guo and S.-M. Hu, *Phys. Rev. Lett.*, 2022, **129**, 163201.
- 137 F. M. J. Cozijn, M. L. Diouf and W. Ubachs, *Phys. Rev. Lett.*, 2023, **131**, 073001.
- 138 C.-L. Hu, V. I. Perevalov, C.-F. Cheng, T.-P. Hua and S.-M. Hu, *J. Phys. Chem. Lett.*, 2020, **11**, 8973–8987.
- 139 C.-L. Hu, J. Wang, T.-P. Hua, A.-W. Liu, Y. R. Sun and S.-M. Hu, *Rev. Sci. Instrum.*, 2021, **92**, 073003.
- 140 I. Langmuir, *J. Amer. Chem. Soc.*, 1912, **34**, 860–877.
- 141 E. E. Witmer, *Phys. Rev.*, 1926, **28**, 1223–1241.
- 142 E. E. Eyler and N. Melikechi, *Phys. Rev. A*, 1993, **48**, R18.
- 143 Y. P. Zhang, C. H. Cheng, J. T. Kim, J. Stanojevic and E. E. Eyler, *Phys. Rev. Lett.*, 2004, **92**, 203003.
- 144 J. Liu, D. Sprecher, C. Jungen, W. Ubachs and F. Merkt, *J. Chem. Phys.*, 2010, **132**, 154301.
- 145 V. I. Korobov, L. Hilico and J.-P. Karr, *Phys. Rev. Lett.*, 2017, **118**, 233001.
- 146 V. A. Yerokhin, K. Pachucki and V. Patkóš, *Ann. Phys.*, 2019, **531**, 1800324.
- 147 S. Patra, M. Germann, J.-P. Karr, M. Haidar, L. Hilico, V. I. Korobov, F. M. J. Cozijn, K. S. E. Eikema, W. Ubachs and J. C. J. Koelemeij, *Science*, 2020, **369**, 1238–1241.
- 148 S. Alighanbari, G. S. Giri, F. L. Constantin, V. I. Korobov and S. Schiller, *Nature*, 2020, **581**, 152–158.
- 149 S. Hannemann, E. J. Salumbides, S. Witte, R. T. Zinkstok, E. J. van Duijn, K. S. E. Eikema and W. Ubachs, *Phys. Rev. A*, 2006, **74**, 062514.
- 150 A. Osterwalder, A. Wüest, F. Merkt and C. Jungen, *J. Chem. Phys.*, 2004, **121**, 11810–11838.
- 151 C. Haase, M. Beyer, C. Jungen and F. Merkt, *J. Chem. Phys.*, 2015, **142**, 064310.
- 152 D. Sprecher, C. Jungen, W. Ubachs and F. Merkt, *Faraday Disc.*, 2011, **150**, 51–70.
- 153 X. Liu, D. E. Shemansky, J. M. Ajello, D. L. Hansen, C. Jonin and G. K. James, *Astrophys. J., Suppl. Ser.*, 2000, **129**, 267–280.
- 154 M. Beyer, N. Hölsch, J. A. Agner, J. Deiglmayr, H. Schmutz and F. Merkt, *Phys. Rev. A*, 2018, **97**, 012501.
- 155 J. Hussels, *PhD thesis*, Vrije Universiteit Amsterdam, 2021.
- 156 R. K. Altmann, L. S. Dreissen, E. J. Salumbides, W. Ubachs and K. S. E. Eikema, *Phys. Rev. Lett.*, 2018, **120**, 043204.
- 157 G. D. Dickenson, M. L. Niu, E. J. Salumbides, J. Komasa, K. S. E. Eikema, K. Pachucki and W. Ubachs, *Phys. Rev. Lett.*, 2013, **110**, 193601.
- 158 P. Wcisło, I. E. Gordon, C.-F. Cheng, S.-M. Hu and R. Ciuryło, *Phys. Rev. A*, 2016, **93**, 022501.
- 159 A. Carrington, I. R. McNab and C. A. Montgomerie, *J. Phys. B: At., Mol. Opt. Phys.*, 1989, **22**, 3551–3586.
- 160 W. Ubachs, *Science*, 2020, **370**, 1033.